


Article

Investigation on Swelling Performance of Oil Sands and Its Impact on Oil Production during SAGD Processes

Xiuyu Wang ^{1,*} , Chuanying Zhang ¹ and Guorui Sun ²¹ College of Petroleum Engineering, China University of Petroleum (Beijing), Beijing 102249, China² College of Petroleum Engineering, Liaoning Petrochemical University, Fushun 113001, China

* Correspondence: wangxiuyu@cup.edu.cn; Tel.: +86-138-1127-0754

Abstract: SAGD (Steam Assisted Gravity Drainage) is used in Canadian fields where there are interlayers that impede steam chamber development and thus impede production. Many experiments have been conducted on the effect of interlayers on oil recovery. However, the swelling characteristics of interlayers under different conditions, as well as the possible clay mineral transformation and particle migration of clay particles at high temperatures, are rarely studied. In this paper, the swelling characteristics of natural oil sands and artificial clay samples were studied by high temperature hydration swelling experiments to obtain a better comparison. The effects of temperature, pressure and solution type on the swelling rate of oil sand were studied. The uniaxial compressive strength of the core in the presence of clay was studied by the scribe test. In addition, before and after the aging test at 220 °C and 2.5 MPa, the clay mineral composition was studied by the X-ray diffraction method, and the mineral transformation was proved. Finally, the impact of clay swelling on oil production is investigated by simulating the particle migration effect while considering the swelling effect. The results show that the swelling rate of oil sand increases with the increment of temperature and the decrement of pressure. The swelling rate of an artificial clay sample in distilled water is the highest, while a 1% KCl + 1% CaCl₂ solution has the best swelling inhibition effect. This study aims to provide new insights into reservoir damage research during SAGD development.

Keywords: oil sands; swelling rate; illite-montmorillonite mixed layer; mineral transformation; particle migration



Citation: Wang, X.; Zhang, C.; Sun, G. Investigation on Swelling Performance of Oil Sands and Its Impact on Oil Production during SAGD Processes. *Energies* **2022**, *15*, 6744. <https://doi.org/10.3390/en15186744>

Academic Editor: Albert Ratner

Received: 24 July 2022

Accepted: 9 September 2022

Published: 15 September 2022

Publisher's Note: MDPI stays neutral with regard to jurisdictional claims in published maps and institutional affiliations.



Copyright: © 2022 by the authors. Licensee MDPI, Basel, Switzerland. This article is an open access article distributed under the terms and conditions of the Creative Commons Attribution (CC BY) license (<https://creativecommons.org/licenses/by/4.0/>).

1. Introduction

SAGD (Steam Assisted Gravity Drainage, SAGD) is a method of injecting steam into the oil reservoir from a vertical well or a horizontal well located above a horizontal production well near the bottom of the oil reservoir. The heated crude oil and steam condensate are removed from the reservoir [1]. SAGD is applied in the oil fields in Canada, and geological testing has revealed the existence of interlayers which hinder the development of steam chambers and affect oil production. The presence of interlayers will reduce the overall permeability of the reservoir and hinder the growth of steam chambers [2–8], which ultimately leads to a recovery reduction in heavy oil reservoirs. Numerical simulation and physical simulation experiments have been used to study the influence of the position of wells relative to barriers on the recovery factor in SAGD development [9–12]. The results show that the barriers in the reservoir will affect the reservoir permeability, especially if the barriers exist between the two horizontal wells. Geologically, the influence of temperature and pressure on the elastoplastic deformation of oil sands is studied through high temperature and high pressure triaxial experiments. Temperature has an important impact on elastoplastic deformation of oil sands, leading to porosity and permeability reduction [13–18]. High temperatures will improve the mobility of asphalt in pore and it has a better effect of extracting asphalt when pressure exists [19].

As stated above, many experiments and mathematical simulations regarding interlayers' impacts on oil recovery have been carried out. However, the swelling characteristics of the interlayers, which are mainly composed of clay, under different conditions and the possible clay mineral transformation under high temperatures are rarely studied. It has been verified by other researchers that the swelling performance of clay will be affected by temperature, and clay may also undergo mineral transformation at temperatures above 185 °C [20]. Montmorillonite with higher expansibility can be generated from kaolinite and quartz in oil sands [21,22]. Clay swelling and possible mineral transformation at high temperatures can cause a further decrease in porosity, which in turn affects recovery in SAGD development. In the face of increasing energy demand, it is necessary to study the swelling characteristics and mechanical strength of oil sands containing a certain amount of swelling clay minerals.

In this paper, the illite-montmorillonite mixed layer was found by scanning electron microscope experiments. The swelling ratio of natural oil sands was studied by hydration experiments. The artificial clay samples were prepared according to the core X-ray diffraction results and used to study the effects of different temperatures, pressures and different types of solutions on the clay's swelling behavior. After one week of aging in a closed container at 220 °C and 2.5 MPa, the mineral transformation of clay was studied by comparing the mineral composition of the samples before and after aging. In order to study the mechanical strength of oil sands, scribe tests were carried out and it was found that the uniaxial compressive strength of the interlayers, which are mostly composed of clay, was 2.5 ksi lower than other parts of the core. The existence of clay in the core was identified by thin slices of rock, and then the particle migration after mineral transformation, which impacts oil production, was simulated and studied by numerical simulation technology. This paper provides new attention for the development of oilfields with interlayers by combining the experimental results of oil sand expansion characteristics with other experimental results and proposes that K^+ and Ca^{2+} can be added to the solution to inhibit the expansion of clay particles.

2. Materials Methods

2.1. Materials

Oil sand samples were from the M oil block in Canada. It is found that kaolinite mainly shows a leaf-like or worm-like morphology, and the illite-montmorillonite mixed layer mainly appears as flocculent forms attached to the surface of particles under scanning electron microscopy [23], as seen in Figure 1.

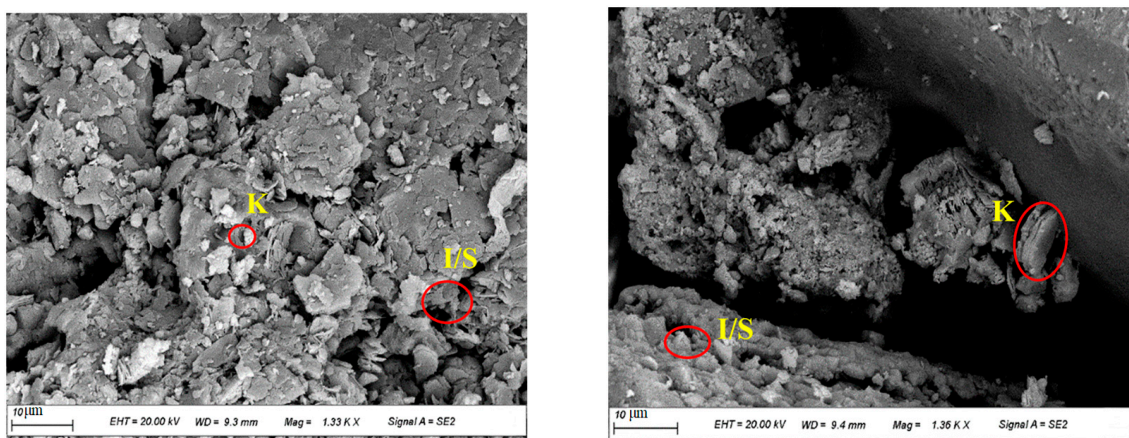


Figure 1. Mineral morphology under scanning electron microscope. Where K is for kaolinite and I/S is for illite-montmorillonite mixed layer.

The solution used in the hydration experiment was made based on the formation water composition, as shown in Table 1. The types and contents of minerals in oil sand

samples are shown in Table 2. X-ray diffraction experiments were carried out on oil sand samples to determine the composition of clay minerals, as shown in Table 3.

Table 1. Ionic and chemical composition of formation water.

Ion Name	Concentration (mg/L)	Pharmaceutical Preparation
Na ⁺ + K ⁺	2330.00	NaCl
Mg ²⁺	27.00	MgCl ₂ ·6H ₂ O
Ca ²⁺	40.00	CaCl ₂
Cl ⁻	2700.00	
SO ₄ ²⁻	600.00	K ₂ SO ₄
HCO ₃ ⁻	1800.00	NaHCO ₃
CO ₃ ²⁻	70.00	Na ₂ CO ₃
Total	7567.00	NaCl

Table 2. Types and contents of mineral in oil sand samples.

Core Number	Mineral Species and Content (%)					Total Clay Mineral (%)
	Quartz (Clastic Quartz + Flint)	Potash Feldspar	Plagioclase	Calcite	Iron Dolomite	
1#	95.1	1	0.9			3
2#	93.2	1.8	1.1	0.4		3.5

Table 3. Relative content of clay mineral.

Core Number	Relative Content of Clay Mineral (%)					Mixed Layer Ratio, S (%)
	S	I/S	I	K	C	
1#		24	15	47	14	7
2#		42	13	34	11	8
3#		32	16	38	14	10

S: smectites; I/S: illite-montmorillonite mixed layer; I: illite; K: kaolinite; C: chlorite; /S: chlorite-montmorillonite mixed layer.

Industry grade clay was used for preparing clay samples to achieve a better comparison effect, according to Table 3. Hydration swelling experiments were used to study different influence factors on clay swelling performance.

2.2. Experimental Setup

The hydration device is HTP-C4 [24], as shown in Figure 2. The N₂ bottle provides the pressure required for the experiment through the Inlet 1 and also provides the pressure for the solution injected into the test bench through the Inlet 2. The air duct is used to maintain the experimental temperature, and the test solution flow controller is used to control the flow rate of the test solution. The test bed controller controls the temperature and switches of the experiment. The pressing sleeve is used to press samples. The data collection system is used to collect the sample expansion rate during the experiment. The precision of measurement is 1%.

2.3. Experimental Procedure

2.3.1. Sample Processing

First, the samples need to be processed, including natural oil sand samples and artificial clay samples, and then experiments are carried out using a high temperature hydration dilatometer [24].

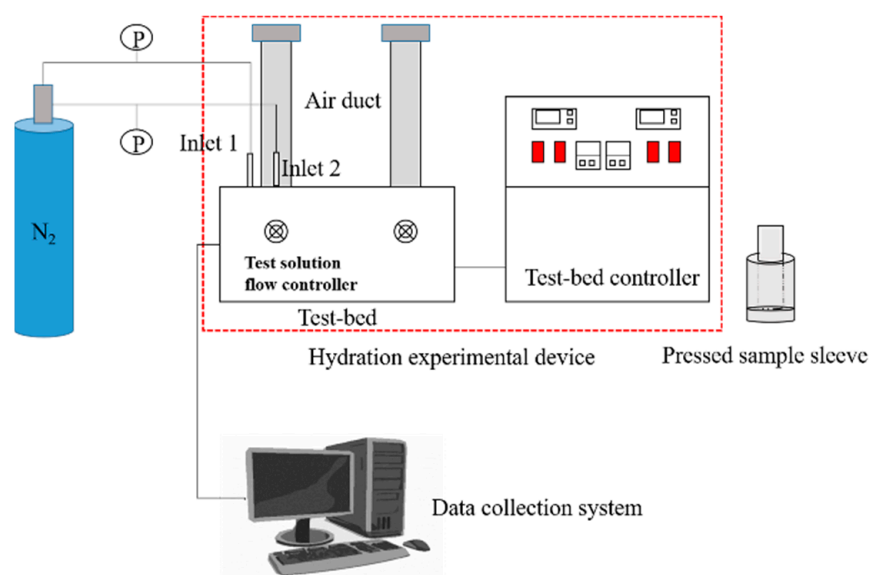


Figure 2. Hydration experimental device.

Since 2# sample has a high montmorillonite content and a relatively large swelling factor, artificial clay samples are prepared according to the clay composition in the 2# core as shown in Table 3. The artificial clay samples are named 2#a to differentiate them from 2#. The contents of kaolinite, chlorite, montmorillonite, and illite are weighed based on a total mass of 10 g (Table 4). Weighed clay is then placed into a plastic cup and stirred thoroughly.

Table 4. Mineral composition of artificial clay samples (2#a).

Clay Type	Weight (g)
Illite	5.164
Kaolinite	3.400
Chlorite	1.100
Montmorillonite	0.336
Total	10.000

2.3.2. Aging Test

The specific steps are:

Put the oil sand debris after oil washing into a high temperature and pressure container;

Add enough formation water to the container to immerse the sample;

Place the container in a drying oven, set the reaction conditions to 220 °C, 2.5 MPa, and the reaction time to 10 days.

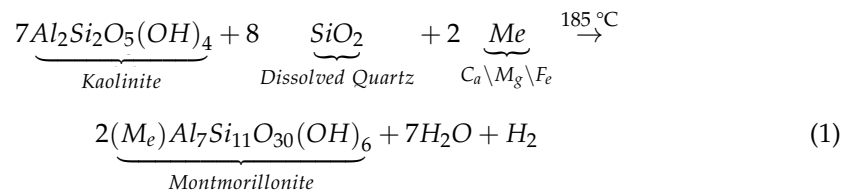
2.3.3. Strength Test of the Core

The nature cores are placed in the core holder, and the compressive strength along the rock scribed direction is obtained by scoring the rock surface [25].

2.3.4. Numerical Simulation Mechanism

CMG (numerical simulation software) is applied to mainly simulate the mineral transformation of clay particles under high temperatures (kaolinite is transformed into an illite-montmorillonite mixed layer) and the particle migration of illite-montmorillonite in the rock core. The REACTION part of the STARS module was used. The main chemical reaction is that part of the kaolinite is converted into montmorillonite at 185 °C (as shown in Equation (1)). The injected steam fluid flows with the detachable montmorillonite particles attached to the rock surface (as shown in Equation (2)), and is “captured” at the pore throat

(as shown in Equation (3)), hindering the flow passage of fluid. The main reaction equation that takes place in this process is [26]:



Under normal conditions, the porosity in the model is the ratio of the pore volume to the total volume of the set grid, but this simulation considers the mineral reaction of the solid phase of the rock, and the generated clay mineral particles migrate with the flow of the fluid. Considering the change of the solid phase, the void porosity is used here.

The total volume of the simulated unit can be determined by V_r (rock matrix volume), V_s (adsorbed solid volume), V_w (water phase volume), V_o (oil phase volume), V_g (gas phase volume), consisting of:

$$V = V_r + V_s + V_w + V_o + V_g \quad (4)$$

The total volume of fluid in the grid is V_f , which is mainly composed of water phase, oil phase, and gas phase volume, namely:

$$V_f = V_w + V_o + V_g \quad (5)$$

The void volume V_v in the grid is the difference between the total volume of the unit and the volume of the solid rock matrix, namely:

$$V_v = V - V_r = V_f + V_s \quad (6)$$

The simulated void porosity can be defined as:

$$\Phi_v = \frac{V_v}{V} \quad (7)$$

According to the above formula, the relationship between the porosity of pores and the solid rock matrix volume can be deduced:

$$\Phi_v = \frac{V_v}{V} = \frac{V - V_r}{V} = 1 - \frac{V_r}{V} = -\frac{1}{V}V_r + 1 \quad (8)$$

3. Experimental Results and Discussion

The hydration swelling experiments are carried out for both oil sand samples and artificial clay samples to better study the clay swelling behavior of oil sand. The test solution used in the experiment is formation water.

3.1. Natural Oil sand Samples

In order to study the influence of the content of illite-montmorillonite mixed layer in oil sands on its swelling characteristics, 1# (I/S: 24%) and 2# (I/S: 42%) cores are selected for their obviously different content of illite-montmorillonite mixed layer. Experimental temperatures are 100 °C, 120 °C, 140 °C, 160 °C, 180 °C, 200 °C, 220 °C, and pressure is kept at 2.5 MPa.

From Figure 3, it can be found that the swelling rate of oil sands increases with the increase in temperature. The swelling rate of 1# is 1.11% at 220 °C while 2# is nearly 4 times that of 1#, reaching 4.2%. It should be mentioned that the total content of clay minerals in 1# core is 3%, while 2# core is 3.5%. The content of the illite-montmorillonite mixed

layer in the clays of 1# and 2# is 24% and 42% separately. The higher the content of the illite-montmorillonite mixed layer in the oil sand, the higher the expansion ratio of the oil sands.

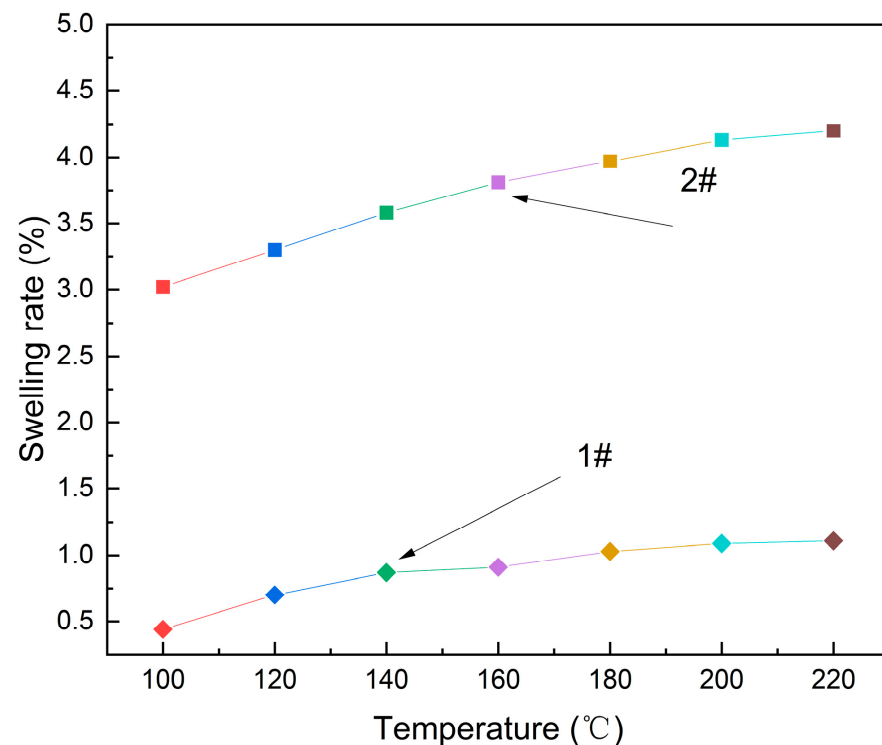


Figure 3. Swelling rater of different oil sands with temperature (1#, 2#).

3.2. Artificial Clay Samples

Because the swelling rates for natural oil sands are low, only less than 5%. To guarantee the same content of illite-montmorillonite mixed layer and for a more obvious comparison effect, artificial clay samples whose mineral content is the same as clays in oil sand sample 2# are used to study influencing factors on swelling performance of oil sands.

3.2.1. Temperature Effect

Effects of different temperatures on hydration swelling of clay samples are investigated at 100 °C, 120 °C, 140 °C, 180 °C, 200 °C, 220 °C, and pressure is 2.5 MPa.

It can be seen from Figure 4 that as temperature increases, the hydration swelling rate of samples gradually increases. As the temperature rises, the swelling property of clay increases, which on one hand causes its own expansion. On the other hand, it can cause more water to enter the layers, further increasing its swelling rate. When the temperature is higher than 180 °C, the swelling rate has a more significant increase. It is deduced that the mineral transformation may happen during the transformation process, kaolinite reacts to form montmorillonite [21], as will be verified later through aging test.

3.2.2. Pressure Effect

The effects of pressure on swelling rate are studied at a temperature of 180 °C. As formation pressure is 3 MPa, and injected steam pressure on field is 2.5 MPa, so 0.1 MPa, 1.0 MPa, 1.5 MPa, 2.0 MPa, 2.5 MPa, 3.0 MPa are set for lab experiments. Results are shown in Figure 5.

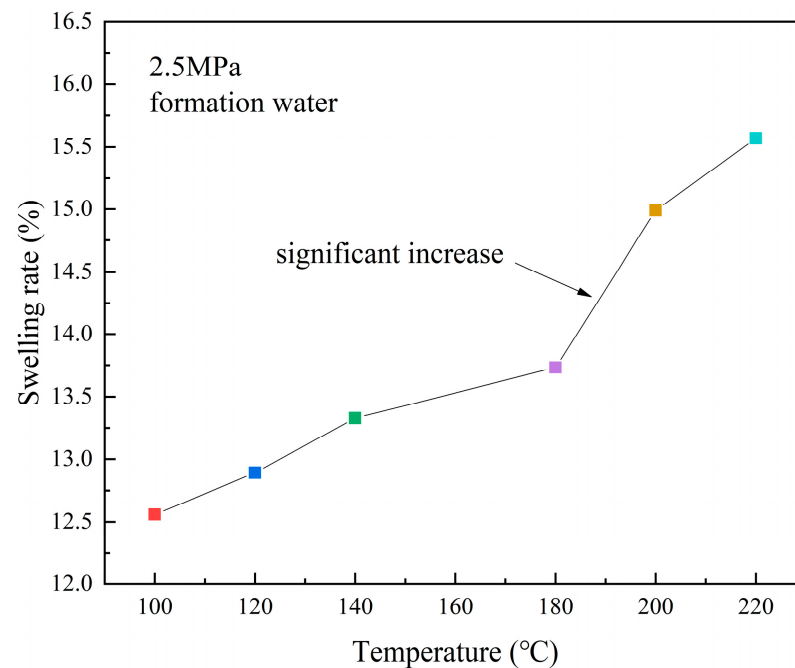


Figure 4. Swelling rate of artificial clay samples with temperature (2#a).

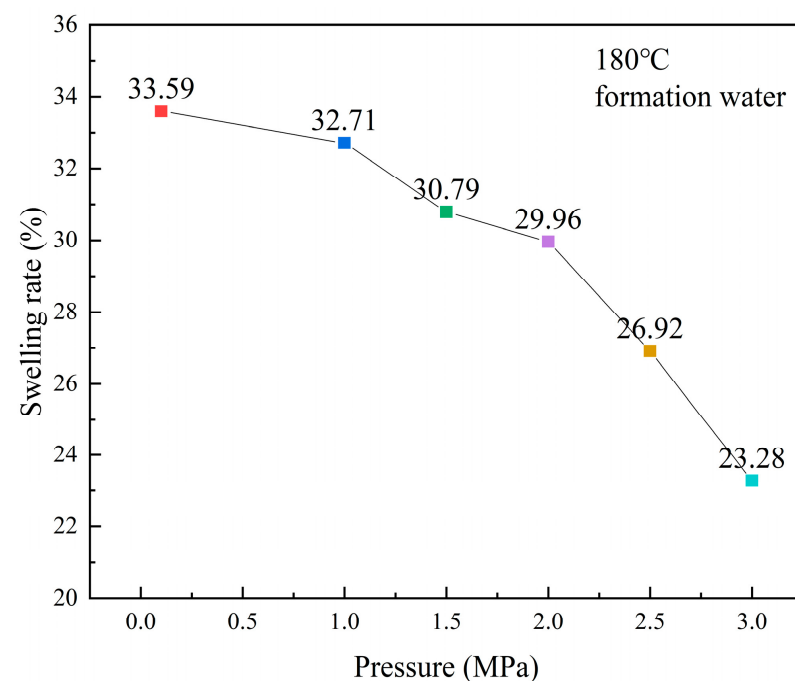


Figure 5. Swelling rate of artificial clay samples with pressure (2#a).

It can be seen from Figure 5 that as pressure decreases, the swelling rate increases. During the experiment, the temperature is first set to 180 °C and the pressure is set to 3.0 MPa. After the swelling rate stabilized, the pressure was decreased to 2.5 MPa, and then the pressure was reduced to 2.0, 1.5, 1.0, and 0.1 MPa accordingly. On one hand, high pressure promotes water molecules to enter into the clay interlayer, which leads to the promotion of hydration. On the other hand, high pressure has a compaction effect on clay [27]. The second effect is more obvious, so when pressure decreases, the compaction effect decreases and the swelling rate increases.

3.2.3. Effect of Different Types of Salt Solutions

Experiments were carried out under 180 °C, 2.5 MPa and different solutions were used, including formation water, 2% KCl, 2% CaCl₂ and 1% KCl + 1% CaCl₂. Distilled water was used for a baseline test.

It can be found from Figure 6 that sample has the highest swelling rate in distilled water, and swelling rate of sample is the lowest in solution of 1% KCl + 1% CaCl₂. Swelling rate of sample is 20.17% with formation water. 2% KCl solution has a certain inhibition effect on clay swelling, which has also been found by other researchers [28]. K⁺ has a better inhibitory effect than Ca²⁺ and mixed 1% KCl and 1% CaCl₂ solution have a best inhibitory effect on clay swelling. Therefore, K⁺ and Ca²⁺ can be appropriately added to steam injected on site to inhibit expansion of clay in formation.

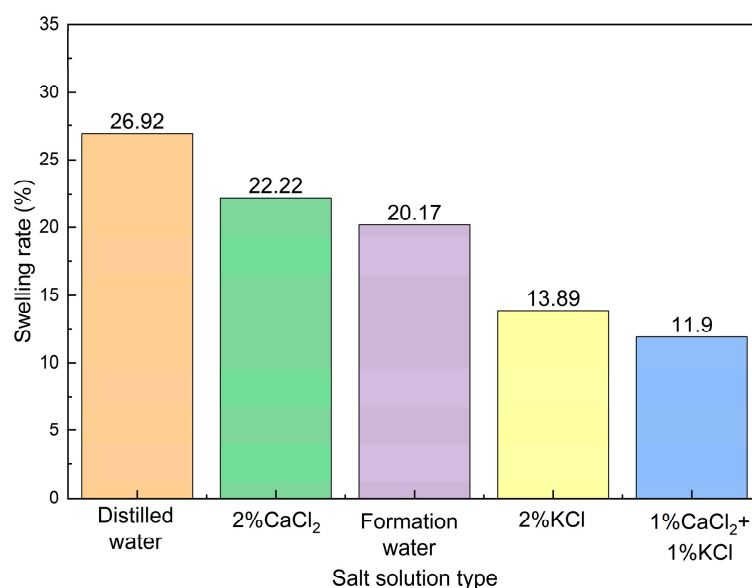


Figure 6. Swelling rate of artificial clay samples with different salt solutions (2#a).

3.2.4. Aging Test

To study the mineral transformation at high temperatures, an aging test [29] was conducted for an artificial clay sample (prepared according to clay composition of another natural oil sand). Mineral composition was analyzed before and after aging the sample in formation water in a sealed container. Results are shown in Table 5.

Table 5. Clay content before and after aging test.

Sample	Relative Content of Clay Mineral (%)					Mixed Layer Ratio (%)		
	S	I/S	It	K	C	C/S	I/S	C/S
Before aging	37		15	48		/		/
After aging		72	28			/	40	/

It can be found that after aging test, kaolinite is completely transformed into an illite-montmorillonite mixed layer. It can be speculated that during SAGD, steam injected may cause the interlayer to swell, reduce formation porosity and thus affect oil production.

3.3. Strength Test of the Core

Scribe test is a new technology used to test rock strength [26]. The results are shown in Figure 7.

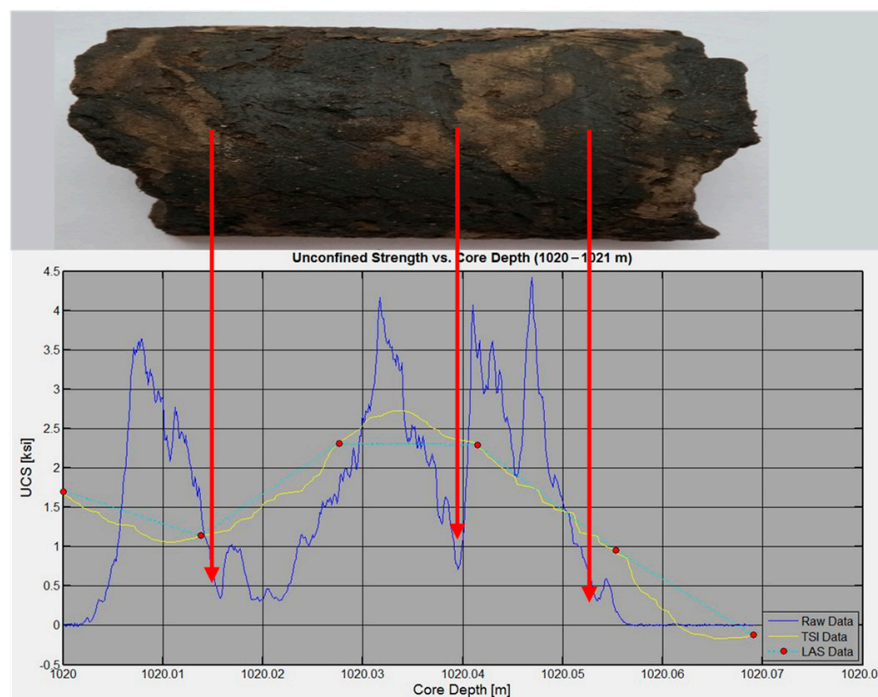


Figure 7. Core scribe test results.

The uniaxial compressive strength of the core is 1~2.5 ksi (1 ksi = 6.84 Mpa), and the strength is low. In order to study whether the compressive strength of the argillaceous lamina in the rock core can correspond to the above experimental results, the particle size of the core was carried out, and it was found that the core with low compressive strength contains relatively more argillaceous.

During the development process, the pressure generated by steam injection may affect its overall structure, especially for the horizon containing argillaceous laminae. Steam injection pressure that is too high may cause micro cracks in the rock stratum, which is beneficial to the development, but for the shallow unconsolidated sandstone oil reservoir, steam injection pressure that is too high may cause the formation to arch up and affect the construction of the ground. Therefore, the pressure of steam injection needs to be considered in the actual development process.

3.4. Clay Particle Migration

3.4.1. Rock Slice Identification

The existence and distribution of clay in the core are studied through the technology of rock slice identification [25]. From Figure 8, the clay can be clearly found and its distribution is uneven. It is no doubt that the porosity will decrease where the clay particles are abundant, affecting the development of the steam chamber. In order to study the clay particle migration, STARS module of CMG is used to simulate the migration of clay particles in the core.

3.4.2. Simulation of Clay Particle Migration

Experiments related to particle transport have been demonstrated in our previous studies [24] and will not be shown again here.

From equation 8, it can be seen that the void porosity is negatively correlated with the rock matrix volume. The larger the rock matrix volume, the lower the void porosity. As montmorillonite generated by the mineral transformation in each grid migrates, the rock matrix volume in each grid changes, and the void porosity also changes. Through the change of the void porosity, the particle migration in the rock can be indirectly analyzed. The simulation results are shown in Figure 9.

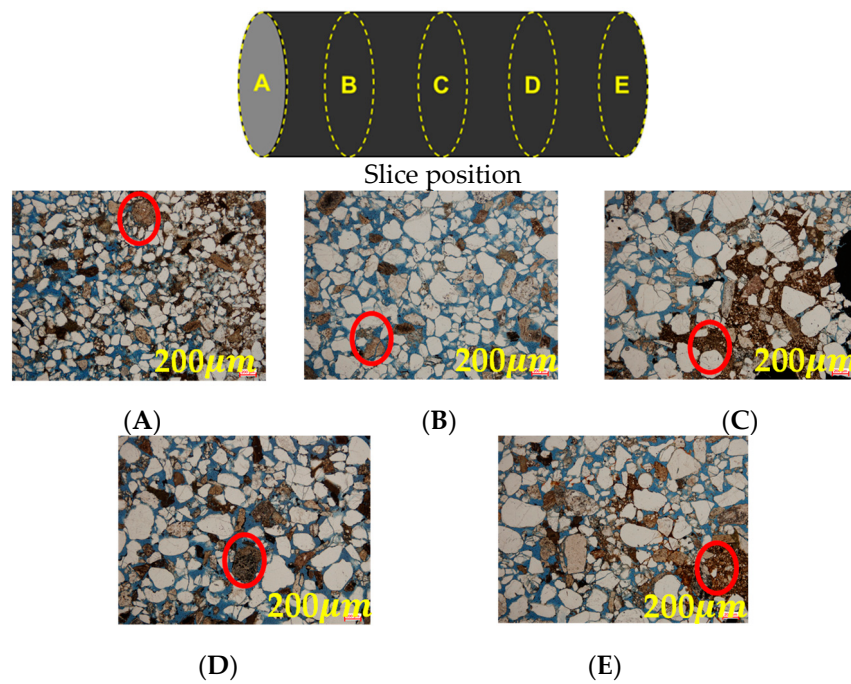


Figure 8. Rock slice images. (A), (B), (C), (D), and (E) are the core slice positions, respectively.

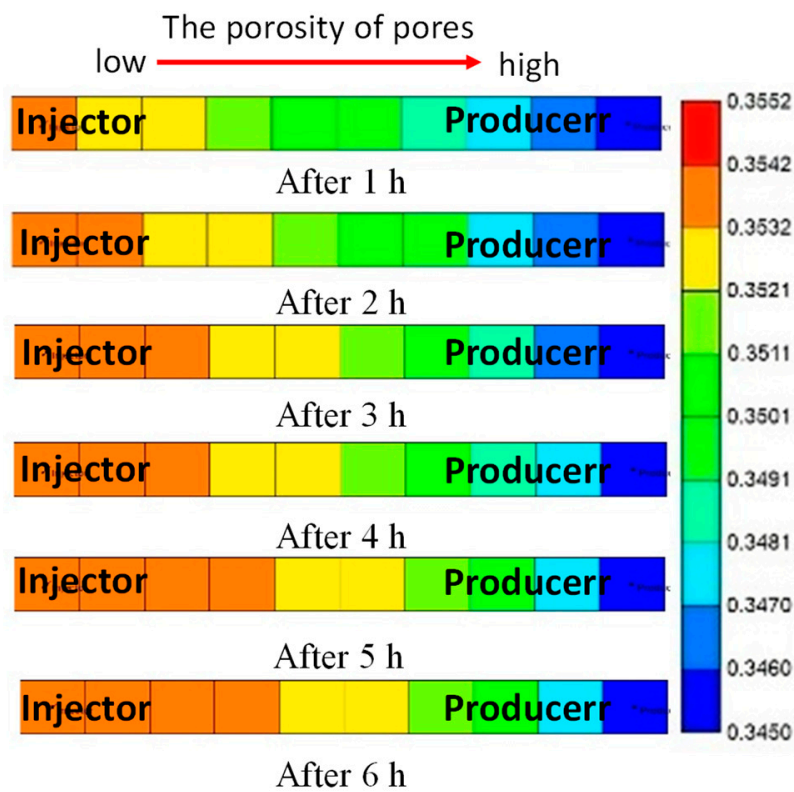


Figure 9. Simulation results of particle migration.

From Figure 9, it can be found that clay particles will migrate in the core. The effect of particle migration on the daily oil production and cumulative oil production within 2 months were then studied by numerical simulation and the results are shown in Figures 10 and 11.

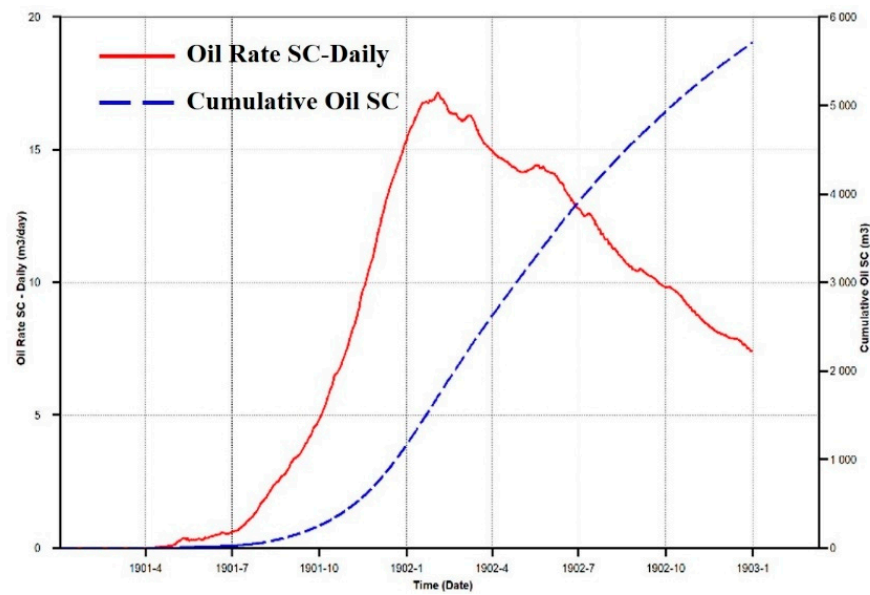


Figure 10. Daily oil production and cumulative oil production (without particle migration).

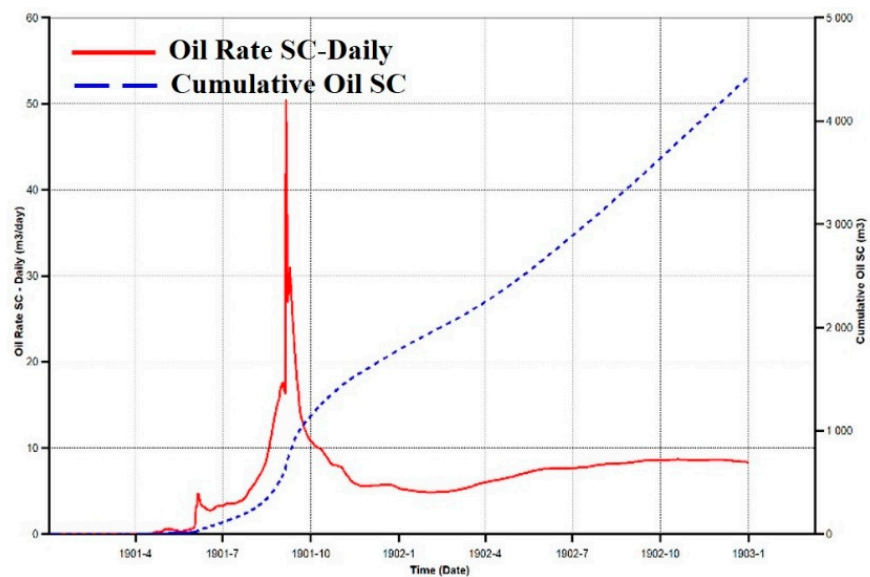


Figure 11. Daily oil production and cumulative oil production (with particle migration).

By comparing the daily oil production under the two simulation conditions, with or without considering particle migration, the daily oil production is higher than that in the absence of the chemical reaction, but after that the daily oil production is lower than without considering particle migration. In comparing the cumulative oil production, it is found that the cumulative oil production without particle migration is 5713.43 m^3 , 23% higher than that when considering particle migration, which is 4424.13 m^3 . The numerical simulation results show that particle migration can affect the matrix distribution and effective porosity inside the rock and ultimately reduce oil recovery.

4. Conclusions

In comparing the expansion rate of different samples, it is found that the higher the content of the illite-montmorillonite mixed layer in the oil sand, the higher the expansion ratio of the oil sands. Temperature and pressure have a great effect on the expansion rate of clay containing. The expansion rate increases with the increase of temperature, while it decreases with the increase of pressure. The experimental results show that the laboratory

swelling ratio of artificial clay samples at 180 °C and 3 MPa is 23.28%, while the swelling ratio of natural oil sands is less than 5% under comparative conditions. It is also found that K^+ and Ca^{2+} have a synergistic inhibitory effect on the swelling rate of the mixed layer, and the 1% KCl + 1% $CaCl_2$ mixed solution has a better inhibitory effect than the solution containing K^+ and Ca^{2+} alone. In addition, in the aging experiment at 220 °C and 2.5 MPa, kaolinite transformed into a mixed layer of illite-montmorillonite. Through the scoring test results, it can be found that the compressive strength of the core with a higher clay content is lower, and the uniaxial compressive strength of the core is 1~2.5 ksi. Numerical simulation results show that the presence of particle migration in the core reduces porosity and ultimately leads to reduced recovery. Therefore, it is recommended to add a certain concentration of K^+ and Ca^{2+} to the SAGD steam, and the possible transformation of the clay at high temperatures should be considered when designing the steam temperature of the onsite development operation.

In order to improve the recovery of heavy oil production, it is necessary to further study the clay swelling effect, and clay inhibitors should be considered to be added in steam during SAGD development.

Author Contributions: Project administration and funding acquisition X.W.; data curation, visualization and writing—original draft preparation, C.Z.; experiment, G.S. All authors have read and agreed to the published version of the manuscript.

Funding: This research received no external funding.

Institutional Review Board Statement: Not applicable.

Informed Consent Statement: Not applicable.

Conflicts of Interest: The authors declare no conflict of interest.

References

1. Cui, G.; Liu, T.; Xie, J.; Rong, G.; Yang, L. A review of SAGD technology development and its possible application potential on thin-layer super heavy oil reservoirs. *Geosci. Front.* **2022**, *13*, 101382. [[CrossRef](#)]
2. Yang, G.; Butler, R.M. Effects of reservoir heterogeneities on heavy oil recovery by steam-assisted gravity drainage. *J. Can. Pet. Technol.* **1992**, *31*, 37–43. [[CrossRef](#)]
3. Chen, Q.; Gerritsen, M.G.; Kovscek, A.R. Effects of reservoir heterogeneities on the steam-assisted gravity-drainage process. *SPE Reserv. Eval. Eng.* **2008**, *11*, 921–932. [[CrossRef](#)]
4. Shin, H.; Choe, J. Shale barrier effects on the SAGD performance. In Proceedings of the SPE/EAGE Reservoir Characterization & Simulation Conference, Abu Dhabi, United Arab Emirates, 19–21 October 2009. [[CrossRef](#)]
5. Zhou, Y.; Xi, C.; Wu, J. Effect of barriers on the SAGD performance result. In Proceedings of the IPTC 2013: International Petroleum Technology Conference, European Association of Geoscientists & Engineers, Beijing, China, 26–28 March 2013. [[CrossRef](#)]
6. Huang, S.; Xiong, H.; Wei, S.; Huang, C.; Yang, Y. Physical simulation of the interlayer effect on SAGD production in Mackay river oil sands. *Fuel* **2016**, *183*, 373–385. [[CrossRef](#)]
7. Li, S.; Yu, T.; Li, Z.; Zhang, K. Experimental investigation of nitrogen-assisted SAGD in heavy-oil reservoirs: A two-dimensional visual analysis. *Fuel* **2019**, *257*, 116013. [[CrossRef](#)]
8. Kumar, A.; Hassanzadeh, H. Impact of shale barriers on performance of SAGD and ES-SAGD—A review. *Fuel* **2020**, *289*, 119850. [[CrossRef](#)]
9. Martinius, A.W.; Fustic, M.; Garner, D.L.; Jablonski, B.V.; Strobl, R.S.; MacEachern, J.A.; Dashtgard, S.E. characterization and multiscale heterogeneity modeling of inclined heterolithic strata for bitumen-production forecasting, McMurray Formation, Corner, Alberta, Canada. *Mar. Pet. Geol.* **2017**, *82*, 336–361. [[CrossRef](#)]
10. Huang, S.; Yang, L.; Xia, Y.; Du, M.; Yang, Y. An experimental and numerical study of a steam chamber and production characteristics of SAGD considering multiple barrier layers. *J. Pet. Sci. Eng.* **2019**, *180*, 716–726. [[CrossRef](#)]
11. Ma, Z.; Leung, J.Y. Leung Integration of data-driven modeling techniques for lean zone and shale barrier characterization in SAGD reservoirs. *J. Pet. Sci. Eng.* **2019**, *176*, 716–734. [[CrossRef](#)]
12. Yin, Y.; Chen, H.; Huang, J.; Feng, W.; Liu, Y.; Gao, Y. Muddy interlayer forecasting and an equivalent upscaling method based on tortuous paths: A case study of Mackay River oil sand reservoirs in Canada. *Pet. Explor. Dev.* **2020**, *47*, 1291–1298. [[CrossRef](#)]
13. Agar, J.G.; Morgenstern, N.R.; Scott, J.D. Geotechnical Behavior of Oil Sands at Elevated Temperatures and Pressures. Ph.D. Thesis, University of Alberta, Alberta, AB, Canada, 1983. [[CrossRef](#)]
14. Kosar, K.M. Geotechnical Properties of Oil Sands and Related Strata. Ph.D. Thesis, University of Alberta, Alberta, AB, Canada, 1989. [[CrossRef](#)]

15. Kerimov, V.; Mustaev, R.; Serkova, U.; Ismailov, J. Geochemical conditions of hydrocarbon accumulation in low-permeability shale sequences. *E3S Web Conf.* **2019**, *98*, 02005. [[CrossRef](#)]
16. Wong, R.C.K. Mobilized strength components of Athabasca oil sand in triaxial compression. *Can. Geotech. J.* **1999**, *36*, 718–735. [[CrossRef](#)]
17. Gao, Y.; Chen, M.; Lin, B.; Jin, Y. Experimental investigation on compressibility of Karamay oil sands under water injection. In Proceedings of the 51st U.S. Rock Mechanics/Geomechanics Symposium, San Francisco, CA, USA, 25–28 June 2017.
18. Lin, B.; Chen, S.; Jin, Y. Evaluation of reservoir deformation induced by water injection in SAGD wells considering formation anisotropy, heterogeneity and thermal effect. *J. Pet. Sci. Eng.* **2017**, *157*, 767–779. [[CrossRef](#)]
19. Gao, Y.; Chen, M.; Pang, H. Experimental investigations on elastoplastic deformation and permeability evolution of terrestrial Karamay oil sands at high temperatures and pressures. *J. Pet. Sci. Eng.* **2020**, *190*, 107124. [[CrossRef](#)]
20. Day-Stirrat, R.J.; Hillier, S.; Nikitin, A.; Hofmann, R.; Mahood, R.; Mertens, G. Natural gamma-ray spectroscopy (NGS) as a proxy for the distribution of clay mineral and bitumen in the Cretaceous McMurray Formation, Alberta, Canada. *Fuel* **2021**, *288*, 119513. [[CrossRef](#)]
21. Thomas, F.B.; Bennion, D.B.; Bennion, D.W.; Hunter, B.E. Experimental and Theoretical Studies of Solids Precipitation from Reservoir Fluid. *J. Can. Pet. Technol.* **1992**, *31*, PETSOC-92-01-02. [[CrossRef](#)]
22. Li, X.; Guo, P.; Li, X.; Zeng, L.; Zhao, W.; Cui, W. Reservoir damage study on thermal recovery of heavy oil reservoir of loose sand. *Pet. Geol. Recovery Effic.* **2000**, *7*, 57–61. [[CrossRef](#)]
23. Khursheed, A.; Osterberg, M. Developments in the design of a spectroscopic scanning electron microscope. *Nucl. Instrum. Methods Phys. Res. Sect. A-Accel. Spectromet. Detect. Assoc. Equip.* **2006**, *556*, 437–444. [[CrossRef](#)]
24. Wang, X.; Zhang, C.; Yu, Y.; Zhou, Y.; Sun, G. Experimental Study on the Variations of Oil Sand Permeability during SAGD Processes. *Energy Fuels* **2021**, *35*, 16506–16514. [[CrossRef](#)]
25. Boon, C.W.; Houlsby, G.T.; Utili, S. A new rock slicing method based on linear programming. *Comput. Geotech.* **2015**, *65*, 12–39. [[CrossRef](#)]
26. Lin, Y.; Gao, S.; Zeng, Y. Evaluation and Analysis of Rock Strength for the Longmaxi Shale. *Pet. Drill. Tech.* **2015**, *43*, 20–25. [[CrossRef](#)]
27. Cao, C.; Pu, X.; Wang, G.; Huang, T. Comparison of shale inhibitors for hydration, dispersion, and swelling suppression. *Chem. Technol. Fuels Oils* **2018**, *53*, 966–975. [[CrossRef](#)]
28. Mao, H.; Qiu, Z.; Huang, W.; Shen, Z.; Yang, L.; Zhong, H. The Effects of Temperature and Pressure on the Hydration Swelling Characteristics of Clay Mineral. *Pet. Drill. Tech.* **2013**, *41*, 56–61. [[CrossRef](#)]
29. Adam, F.; Ali, T.; Paula, B.; Steven, B. Synergy between Commodity Molecules and Nanoparticles as Steam Mobility Control Additives for Thermal Oil Recovery. In Proceedings of the SPE Annual Technical Conference and Exhibition, Virtual, 26–29 October 2020. [[CrossRef](#)]